University of Maribor Press

DOI: https://doi.org/10.18690/um.fov.5.2026.4
ISBN: 978-961-299-160-9

Financing Green Solutions: Asset Returns and Tail Risks

Eugenijus Gabrielius Ivanauskas,
Liepa Urbonaitė, and
Saulius Jokubaitis

Abstract
The translation of green technologies from theoretical potential to industrial adoption hinges on the stability of the financial mechanisms that fund them. This Chapter investigates the risk dynamics and dependence structures of the Green financial ecosystem, comprising Green Bonds, Clean Energy ETFs, and Carbon Credits. Employing a rolling-window ARMA-GARCH-Vine Copula framework we map the evolving topology of sustainable finance and test the "decoupling hypothesis". The analysis reveals that while Green Bonds have successfully decoupled and act as effective portfolio diversifiers, Clean Energy equities remain deeply integrated with broad market risks, functioning as a centralised "hub" for volatility transmission. We further identify a distinct structural shift around mid-2024, where with the fade of the post-pandemic volatility the market network stabilises into an R-Vine structure that transmits shocks more efficiently. Finally, we assess the viability of clean cryptocurrencies, finding them structurally incompatible with institutional hedging strategies due to extreme tail-risk dependence.

Keywords: sustainable finance; vine copulas; ARMA-GARCH models; volatility transmission; risk modelling; tail dependence.

Eugenijus Gabrielius Ivanauskas
Vilnius University, Institute of Applied Mathematics, Naugarduko str. 24, LT-03225, Vilnius, Lithuania
e-mail: gabrielius.ivanauskas@mif.stud.vu.lt,
Liepa Urbonaitė
Vilnius University, Institute of Applied Mathematics, Naugarduko str. 24, LT-03225, Vilnius, Lithuania
e-mail: liepa.urbonaite@mif.stud.vu.lt,
Saulius Jokubaitis
Vilnius University, Institute of Applied Mathematics, Naugarduko str. 24, LT-03225, Vilnius, Lithuania
e-mail: saulius.jokubaitis@mif.vu.lt

1 Introduction

Driven by rapid technological innovation, the scientific community continues to develop viable solutions to the climate crisis. Yet, the translation of these scientific breakthroughs from theoretical potential to widespread industrial adoption hinges on a critical enabler: capital. The central question facing the green transition is no longer just *what* technologies we need and can create, but *how* we can finance both their research and the deployment at the necessary scale.

Ideally, this financial process should be a frictionless, seamless flow of global capital into sustainable projects. In reality, however, the financial instruments that fund these solutions are complex, volatile, and deeply interconnected with the very fossil-fuel systems they aim to replace. If investors perceive uncontrolled risk or hidden contagion channels, the cost of capital spikes, as all that risk is priced in as a premium, and the deployment of green technology stalls. Consequently, the success of every innovation proposed in this chapter hinges on a robust understanding of the financial mechanisms that underpin them. If left unmanaged, financial risk forces capital providers to demand prohibitive risk premiums or exit the sector entirely, leaving the market open to purely speculative volatility. This in turn creates a perfect environment for liquidity crises and frozen credit lines, ultimately threatening to bankrupt even the most scientifically promising green ventures before they can reach industrial scale.

The purpose of this chapter is to eliminate this friction. By rigorously mapping the returns, volatility and tail-risk transmission of green financial assets we aim to provide the risk-management blueprint necessary to keep the capital flowing. We move beyond the feasibility of green solutions to assess their financial feasibility, distinguishing how these assets behave in calm markets versus periods of systemic shocks.

1.1 Regulatory drivers and market growth

In recent years, the financial sector has found itself in a strong position to support the shift toward a greener economy. The growing demand for green assets isn't just the result of investors paying more attention to Environmental, Social, and Governance (ESG) principles. A major driver is the rigorous regulatory environment. Policies such as carbon pricing and subsidies for renewable energy have shifted investment trends: they raise the cost of holding high-carbon assets and make sustainable projects more financially attractive [48]. Moreover, the development of market infrastructure has been essential in limiting the risk of greenwashing [19]. Efforts like the Climate Bonds Initiative's Green Bond Dataset Methodology [17] and the EU's Sustainable Finance Disclosure Regulation (SFDR) [7] have introduced clearer, standardized classifications. These frameworks make it easier to verify the credibility of green assets, improve transparency, and strengthen institutional confidence.

Although theory suggests that green assets may offer diversification benefits, empirical results are mixed when it comes to their hedging performance during systemic crises [9]. As a result, it is important to examine tail dependence between sustainable

and traditional assets (e.g. stocks and commodities), together with possible spillover effects and their implications for risk.

1.2 Green asset classes

We distinguish four essential financial flows. First, there is the emissions trading system (ETS), designed to manage carbon emissions and phase out old technologies. ETS sets a declining cap on total greenhouse gas emissions and issues tradable allowances, often called carbon credits. Regulated companies must monitor and report emissions each year and submit allowances equal to those emissions. In case of a breach, they face fines, must buy and submit the missing allowances and the breach is published. Allowances are mostly auctioned, with some free allocation to reduce carbon leakage. Firms can buy and sell allowances, so those that cut emissions can sell surplus units while higher emitters buy more. Because the supply of allowances is policy-controlled and falls over time, companies have an incentive to invest in cleaner technologies and to sell surplus credits as prices rise. ETSs typically cover power generation, heavy industry and parts of transport, however in the EU, for example, coverage is expanding to shipping, with a separate system for buildings and road transport. Trading of such allowances improves liquidity and ideally guides investment and faster transition towards lower-carbon technologies. Unlike a carbon tax, which fixes the price per tonne and leaves total emissions uncertain, an ETS fixes the cap and lets the market set the price, so cuts happen where they cost least [37].

Second, the green bond market is designed to finance sustainable, environmentally focused projects. This type of investment has attracted investor interest, supported by diversification benefits and robust transparency. Typically, the funds are used to finance improvements in transport infrastructure, agricultural production, renewable energy generation, and related climate-oriented investments. An important distinction can be made between a “green bond” and a “climate bond”. While both are similar, the latter is designed specifically to finance initiatives that are related to climate change, such as reducing carbon emissions and preventing pollution. Environmental bonds can be issued by various types of issuers, including supranational organisations, national governments, sub-national authorities (such as regions and cities) and corporations. [10].

Third, there are ETFs, stocks and other instruments that use funds for green companies and projects. These often focus on renewable energy, recycling, waste reduction, pollution control, sustainable transport and other green activities. To identify green companies, investors usually use ESG ratings. MSCI, a global provider of investment research and indices, provides such ratings and evaluates companies from CCC to AAA [43]. Examples of ETFs that use ESG or clean energy criteria include iShares ESG MSCI USA Leaders ETF (SUSL), Vanguard ESG U.S. Stock ETF (ESGV), iShares Global Clean Energy ETF (ICLN). These markets are growing fast, which can also increase price swings and speculative risk.

Finally, we consider an emerging asset class of clean cryptocurrencies. While these digital assets are generally not labelled as green, they are often regarded as more climate-friendly due to (unlike Bitcoin, which relies on a high-energy mining process)

the energy-efficient proof-of-stake protocol that significantly reduces electricity consumption and carbon footprint [26, 42, 56]. One hypothesis is that such cryptocurrencies exhibit different tail-risk characteristics and stronger connectedness with the green economy than traditional cryptocurrencies.

1.3 Systemic risk and the decoupling hypothesis

To attract and commit long-term investments to environmental projects, investors and policymakers need to understand how the risks of these assets change under different market conditions, especially how they behave together during extreme events. As green assets become more widely traded, they are more exposed to spillovers when shocks in speculative markets spread to connected markets. During economic turmoil, market interconnections can cause sell-offs and price drops that destabilise sustainable portfolios. In theory, diversification across green instruments should help counter these effects.

The purpose of this study is to empirically assess these dynamics by modelling the univariate risk and multivariate dependence structures of green financial instruments under both calm and volatile conditions. To capture the drivers of global market stress, the analysis incorporates key external variables, including industrial and precious metal futures (copper, gold), broad equity market trends (S&P 500) and energy commodity shocks (natural gas). The aim is to span a set of specific dimensions of the global economic environment. We consider Gold futures (GCF) to act as a proxy for safe-haven demand and inflationary expectations, allowing us to control for flight-to-safety episodes during market turmoil [5, 38]. Conversely, copper futures (HGF), often referred to as "Doctor Copper", serve as a barometer for global industrial activity and business cycle fluctuations [60]. Crucially, it is also one of the key material inputs needed for green technology development (e.g., electric vehicles, wind turbines), creating a physical link between commodity prices and renewable sector profitability [29]. The S&P 500 represents the baseline for global equity risk sentiment, capturing the broad market movements. Finally, while Natural Gas (TTFF) was the central driver of the 2022 crisis, our analysis treats it as a "stress test" variable to evaluate how the market structure adapts to energy shocks. As a marginal price-setter for electricity in many markets [63], the shocks of natural gas price directly impact the cost competitiveness of renewable energy alternatives. This makes the variable crucial for analysing the decoupling hypothesis (see, e.g., [41, 53]).

The decoupling hypothesis posits that the performance of green assets should increasingly diverge from that of the traditional carbon-heavy markets as the transition to a low-carbon economy intensifies [64]. The expected separation is driven by two fundamental drivers. First, while the traditional energy markets are governed by commodity supply shocks and geopolitical events, the green asset returns should be increasingly influenced by technological innovation, regulatory requirements and long-term policy support [13, 27, 39]. If this hypothesis holds, green assets serve as not only attractive instruments for capital allocation, but as effective hedges against carbon transition risk [55]. However, recent evidence suggests that financial contagion and shared

macroeconomic factors may re-couple these sectors during periods of systemic stress [3, 54].

Green bonds typically demonstrate a weak and time-varying correlation with traditional energy markets, indicating partial decoupling from non-climate-friendly assets [45, 49]. However, these relationships are highly dynamic and tend to spike during periods of systemic stress, such as the Global Financial Crisis, the COVID-19 pandemic, or regimes of extreme downside risk. During such stress periods, the interdependencies across assets strengthen, making joint extreme losses more likely and causing diversification benefits to decrease [14, 62]. This dependence differs across energy types: green bonds show an extreme negative tail dependence with oil and coal during crises but a positive dependence with natural gas, likely because both are seen as ways to limit environmental harm [45, 49]. Since green bonds do not closely follow the price swings of traditional energy, they can offer diversification benefits and some hedging potential, particularly for short-term investors seeking protection from energy market volatility [45, 49].

The green bond market is linked to broader financial sectors through spillover effects, with volatility spillovers occurring even when average correlations are low. While broad equity and energy markets tend to have minor direct influence on green bond prices, specific sectors, such as renewable energy equities, play a more important role in transmitting shocks to the green bond market [44, 66]. In the energy sector specifically, crude oil and green bonds are linked through asymmetric spillovers: negative return shocks in oil markets can increase green bond volatility, while green bond shocks may reduce oil market volatility as investors shift away from energy assets [44, 59]. These dynamics are highly time-dependent, as the connection with oil is typically weak in the short-run but strengthens in the long-run due to industrial competition for capital [44]. Furthermore, green bonds receive significant price spillovers from traditional corporate and treasury fixed-income markets, making them poor diversifiers for investors already holding traditional bonds [53, 66]. Carbon markets and cryptocurrencies also play a role in this ecosystem, with cryptocurrencies acting as a notable source of volatility for green bonds in bearish market conditions [59, 66].

To capture these potential non-linear dynamics and complex structures, we use an ARMA–GARCH–Vine–Copula modelling framework [14, 30]. This approach first models the marginal return dynamics and conditional volatility of each asset using ARMA–GARCH type specifications, such as GJR–GARCH, EGARCH, PARCH or others for asymmetric volatility and leverage effects [14, 51, 52, 62]. The dependence structure is then modeled using vine copulas [1, 8, 14, 15, 31], which provide the flexibility needed to capture asymmetric tail dependence and to identify specific causality between assets. The frequent use of these models in previous green finance studies supports their suitability for analyzing volatility, tail risk, and dependence in green financial markets [14, 51, 62].

While alternative methodologies such as DCC-GARCH [21, 57] or wavelet coherence [34, 35, 61] are widely used to assess time-varying connectedness, they often rely on restrictive assumptions regarding the joint distribution of returns. We consider the ARMA-GARCH-Vine-Copula approach more suitable for this analysis as it provides a flexible modelling framework for understanding tail risk without imposing strong symmetry assumptions in the dependence structure. This flexibility allows us to identify

whether green assets maintain their diversification properties when the market is under specific stress from energy commodity shocks.

Our contribution to the existing literature is threefold. First, we model the univariate volatility dynamics of these assets, accounting for the heavy tails and leverage effects characteristic of new financial markets. Second, we employ a vine copula framework to map the multivariate dependence structure. This approach allows us to move beyond simple linear correlations and identify tail dependence: the likelihood of simultaneous extreme losses. Finally, by challenging the decoupling hypothesis we find that the Green Bonds have successfully decoupled and are acting as effective portfolio diversifiers, while the clean energy equities remain deeply integrated with broad market risks. Furthermore, we identify a lagging structural shift, observed in our rolling window experiments around mid 2024. As the memory of the energy crisis fades, the green financial network has hardened, becoming less volatile on the average, but structurally more centralised around specific hubs (Clean Energy ETFs), allowing shocks to transmit faster than before.

2 Methodology

For each asset $j = 1, \ldots, d$, a univariate return series is constructed using daily continuously compounded returns:

$$r_{j,t} = \ln(P_{j,t}) - \ln(P_{j,t-1}),$$

where $P_{j,t}$ denotes the closing price of asset j at time t.

To capture time-varying volatility, several GARCH-type models are estimated for each return series. All models follow the general structure:

$$r_{j,t} = \mu_j + \varepsilon_{j,t}, \qquad \varepsilon_{j,t} = \sigma_{j,t} z_{j,t}, \qquad \mu_j \in \mathbb{R},$$

where $\sigma_{j,t}$ is the conditional standard deviation and $z_{j,t}$ is an i.i.d. standardized innovation.

Since empirical asset returns typically exhibit heavy tails and excess kurtosis that are not adequately captured by the normal distribution [2, 33, 67], we assume that the standardized innovations follow a Student's t-distribution [11] where the degrees of freedom ν are estimated via maximum likelihood.

In this chapter we consider the following volatility models: GARCH, iGARCH, EGARCH, GJR-GARCH, APARCH, csGARCH. The first moments were modelled by using ARMA models.

The adequacy of the model is assessed in two stages. At first, standardized residuals are evaluated using the Ljung–Box and ARCH–LM tests to examine the remaining autocorrelation and conditional heteroskedasticity. Secondly, implied Value-at-Risk forecasts are validated using the Kupiec unconditional coverage test, Christoffersen conditional coverage test, the independence test, and the Basel Traffic Light test.

The baseline GARCH(1,1) model [12], which captures short-term memory and volatility clustering, is defined by eq. (1):

$$\sigma_{j,t}^2 = \omega_j + \alpha_j \varepsilon_{j,t-1}^2 + \beta_j \sigma_{j,t-1}^2. \tag{1}$$

While this baseline provides a foundational framework, our preliminary testing revealed that models incorporating leverage effects (GJR-GARCH) or long-run volatility components (csGARCH) provided a superior fit for our data. Consequently, for the sake of brevity, the detailed mathematical definitions and empirical results presented in the following sections focus strictly on these best-performing frameworks.

Value-at-Risk (VaR) forecasts are computed directly from the conditional mean and volatility:

$$\mathrm{VaR}_{j,t+1}(\alpha) = \widehat{\mu}_{j,t+1} + \widehat{\sigma}_{j,t+1} q_\alpha,$$

where q_α is the α-quantile of the Student's t-distribution. We consider two confidence levels, namely the 95% and the 99% VaR.

2.1 GJR-GARCH

The GJR-GARCH model of Glosten, Jagannathan, and Runkle [24] extends the standard GARCH framework by allowing asymmetric volatility responses to positive and negative shocks. This asymmetry, known as the leverage effect, captures the empirically observed phenomenon that negative return innovations tend to increase volatility more than positive ones.

The conditional variance equation is given by:

$$\sigma_{j,t}^2 = \omega_j + \sum_{k=1}^{q} \left(\alpha_{j,k} \varepsilon_{j,t-k}^2 + \gamma_{j,k} I_{j,t-k} \varepsilon_{j,t-k}^2 \right) + \sum_{k=1}^{p} \beta_{j,k} \sigma_{j,t-k}^2, \tag{2}$$

where the indicator function $I_{j,t-k}$ is defined as:

$$I_{j,t-k} = \begin{cases} 1, & \varepsilon_{j,t-k} \le 0, \\ 0, & \varepsilon_{j,t-k} > 0. \end{cases} \tag{3}$$

The parameter γ_k measures the leverage effect; $\gamma_k > 0$ implies stronger volatility responses to negative shocks.

2.2 csGARCH model

The model proposed by Lee and Engle decomposes the conditional variance into two distinct components: a permanent component and a transitory component [22]. This

decomposition allows for the analysis of both long- and short-term volatility dynamics in financial assets. The permanent component, denoted by $m_{j,t}$, evolves over time and replaces the constant intercept of the standard GARCH model with a time-varying term that follows first-order autoregressive dynamics. The transitory component is defined as the deviation of the conditional variance from its long-term trend, given by

$$\sigma_{j,t}^2 - m_{j,t}.$$

The model can be written as:

$$\sigma_{j,t}^2 = m_{j,t} + \sum_{k=1}^{q} \alpha_{j,k} \left(\varepsilon_{j,t-k}^2 - m_{j,t-k} \right) + \sum_{k=1}^{p} \beta_{j,k} \left(\sigma_{j,t-k}^2 - m_{j,t-k} \right), \tag{4}$$

$$m_{j,t} = \omega_j + \rho_j m_{j,t-1} + \phi_j \left(\varepsilon_{j,t-1}^2 - \sigma_{j,t-1}^2 \right). \tag{5}$$

To ensure that the conditional variance remains non-negative, the model imposes parameter restrictions as described in [22]. In particular, the sum of the GARCH parameters α and β must be less than one, and the persistence parameter ρ governing the permanent component must satisfy $\rho < 1$. Together, these conditions guarantee the stationarity and stability of both the transitory and permanent volatility components.

2.3 eGARCH model

The exponential GARCH (eGARCH) model introduced by Nelson [47] can be written as:

$$\ln\left(\sigma_{j,t}^2\right) = \left(\omega_j + \sum_{k=1}^{m} \zeta_{j,k} v_{j,k,t} \right) + \sum_{k=1}^{q} \left(\alpha_{j,k} z_{j,t-k} + \gamma_{j,k} \left(|z_{j,t-k}| - \mathbb{E}|z_{j,t-k}| \right) \right) + \sum_{k=1}^{p} \beta_{j,k} \ln\left(\sigma_{j,t-k}^2\right), \tag{6}$$

where $z_{j,t} = \varepsilon_{j,t}/\sigma_{j,t}$ denotes the standardized innovations. The constant term ω_j captures the long-term level of logarithmic conditional variance, while the term $\zeta_{j,k} v_{j,k,t}$ allows the inclusion of additional variables that may influence volatility dynamics, such as macroeconomic or market-specific factors. When no additional variables are considered, this term is typically omitted.

A key advantage of the eGARCH model is that it does not require parameter restrictions, since the conditional variance is modelled in logarithmic form. This guarantees the positivity of the variance by construction. Using the logarithm of volatility also means that shocks affect volatility in relative terms rather than absolute levels. As a result, very large shocks do not cause excessively large increases in the conditional variance, leading to a more stable reaction to extreme market movements.

The parameters $\alpha_{j,k}$ and $\gamma_{j,k}$ describe how shocks influence volatility. The coefficient $\alpha_{j,k}$ captures asymmetric effects, allowing negative and positive shocks to have different impacts on volatility. The parameter $\gamma_{j,k}$ measures the effect of the size of shocks and determines how strongly volatility responds to large unexpected returns, regardless of their sign.

The persistence of volatility in the eGARCH model is mainly determined by coefficients $\beta_{j,k}$, which control how long the impact of shocks remains in the variance process. Due to the logarithmic specification, the persistence of volatility is more flexible than in standard GARCH models, as the speed at which shocks decay depends on the estimated parameters rather than fixed constraints.

2.4 Copulas

2.4.1 Sklar's theorem

The copula approach is based on Sklar's Theorem [58]. Let F be a d-dimensional joint distribution function with marginals $F_1, \ldots, F_d$. Then there exists a copula $C : [0,1]^d \to [0,1]$ such that:

$$F(x_1, \ldots, x_d) = C\big(F_1(x_1), \ldots, F_d(x_d)\big), \quad (x_1, \ldots, x_d) \in \mathbb{R}^d. \tag{7}$$

Archimedean copulas
Archimedean copulas are constructed using a generator function ϕ:

$$C(u_1, \ldots, u_d) = \phi^{-1}\left(\phi(u_1) + \cdots + \phi(u_d)\right), \tag{8}$$

where $u_i = F_i(x_i)$ are the marginal probabilities in $[0,1]$, $\phi : [0,1] \to [0,\infty)$ is a strict Archimedean generator function (continuous, strictly decreasing, convex), ϕ^{-1} is the pseudo-inverse of the generator.

Elliptical copulas
Elliptical copulas are derived by inverting Sklar's theorem for elliptical distributions.

$$C(u_1, \ldots, u_d) = F\left[F_1^{-1}(u_1), \ldots, F_d^{-1}(u_d)\right], \tag{9}$$

where F is a joint elliptical distribution function (e.g., Multivariate Normal or Student's t), F_j^{-1} is the inverse CDF of the univariate marginals of F.

2.5 Vine copula structures

To model dependence of the residuals of univariate volatility models we use the vine copula approach. Unlike Archimedean copulas, which typically rely on a single parame-

ter and can be restrictive in higher dimensions, vines allow each variable pair to be fitted with an appropriate copula family, providing flexibility, tail-dependence modelling and asymmetry. Vine copulas let different variable pairs be modelled with different copula families, providing substantial modelling flexibility. They build pair-copula constructions that decompose a multivariate distribution into bivariate components, with variables connected across a sequence of trees to represent dependence. The key property is that the joint density can be factorised into products of conditional densities [1, 8, 14, 15, 31]. Below we define all relevant notation.

2.5.1 C-Vine (Canonical vine)

The C-Vine structure is a "star-like" dependency where one pivot variable drives the dependence of the others. Joint density function is denoted as follows:

$$f(x_1,\ldots,x_d)=\prod_{k=1}^{d} f_k(x_k)\times\prod_{j=1}^{d-1}\prod_{i=1}^{d-j} c_{j,j+i|1:\cdots:j-1}\left(F(x_j|\mathbf{x}_{1:j-1}),F(x_{j+i}|\mathbf{x}_{1:j-1})\right), \tag{10}$$

where $f_k(x_k)$ are the marginal densities, $c_{j,j+i|\ldots}$ represents the pair-copula density between variable j and $j+i$, conditional on previous variables, $1:\cdots:j-1$ denotes the set of conditioning variables $\{x_1,\ldots,x_{j-1}\}$. In a C-Vine, variable 1 is the root node for the first tree, variable 2 for the second, etc.

2.5.2 D-Vine (Drawable vine)

The D-Vine structure assumes a "line-like" or sequential dependency. A D-vine emerges when the dependence structure is sequential, with no dominant "hub" variable, meaning that each variable mainly depends on its neighbours rather than on a central node. Joint density function denoted as:

$$f(x_1,\ldots,x_d)=\prod_{k=1}^{d} f_k(x_k)\cdot\prod_{j=1}^{d-1}\prod_{i=1}^{d-j} c_{i,i+j|i+1:\cdots:i+j-1}\left(F(x_i|\mathbf{x}_{i+1:i+j-1}),F(x_{i+j}|\mathbf{x}_{i+1:i+j-1})\right) \tag{11}$$

where the conditioning set $i+1:\cdots:i+j-1$ represents the variables strictly "between" i and $i+j$ in the sequence. For the first tree ($j=1$), the conditioning set is empty, giving unconditional pair copulas $c_{i,i+1}$. D-vine is a special case of R-vine structure.

2.5.3 R-Vine (Regular vine)

The R-Vine is the most general structure, defined by a sequence of trees. Joint density is denoted as:

$$f(x_1,\ldots,x_d) = \prod_{k=1}^{d} f_k(x_k) \times \prod_{i=1}^{d-1} \prod_{e\in E_i} c_{j(e),k(e)|D(e)} \left(F(x_{j(e)}|\mathbf{x}_{D(e)}), F(x_{k(e)}|\mathbf{x}_{D(e)})\right) \tag{12}$$

where E_i is the set of edges in tree T_i, $e = \{j(e), k(e)\}$ describes the two variables connected by the edge, $D(e)$ is the conditioning set for edge e (the variables needed to make the pair conditional).

2.5.4 Copula families

In this study, the candidates for the pair-copulas are restricted to a specific selection of Elliptical (Gaussian, Student's t) and Archimedean (Gumbel, Clayton) families (listed in Table 1). This selection is designed to provide a full coverage of potential dependence structures, specifically regarding tail behaviour, symmetry, and direction. The Gaussian copula is included as a benchmark for linear, symmetric dependence, suitable for capturing correlation in the centre of the distribution. In contrast, the Student's t copula is employed to capture symmetric fat tails, allowing for the modelling of simultaneous extreme events in both directions.

To account for asymmetric dependence, the Clayton and Gumbel families are used. The standard Clayton copula models lower tail dependence, while the Gumbel copula captures upper tail dependence. Furthermore, we extend the copulas set to include the rotated versions (90°, 180°, and 270°) of these Archimedean families. This extension is critical because standard Archimedean copulas are restricted to positive dependence, the 90° and 270° rotations allow the vine model to capture negative dependence structures. Additionally, the 180° rotations (or survival copulas) offer flexible forms for tail dependence in the opposite direction of the standard form, such as using a Survival Gumbel to model lower tail dependence with a different shape than the Clayton. Collectively, this set ensures the model selection algorithm can flexibly adapt to data exhibiting no tail dependence, symmetric tail dependence, or asymmetric dependence in any direction.

In the general case for a bivariate copula $C(u, v)$, the rotated versions are defined as: $C_{90°}(u, v) = v - C(1 - u, v)$, $C_{180°}(u, v) = u + v - 1 + C(1 - u, 1 - v)$, $C_{270°}(u, v) = u - C(u, 1 - v)$. See for example [32, 46] as reference. Here $u, v \in (0, 1)$ denote uniform marginal variables obtained via the probability integral transform. In Table 1 $\Phi(\cdot)$ and $\Phi^{-1}(\cdot)$ represent the standard normal cumulative distribution function and its inverse, while $\Phi_\rho(\cdot, \cdot)$ denotes the bivariate standard normal distribution with correlation parameter ρ. Similarly, $t_\nu(\cdot)$ and $t_\nu^{-1}(\cdot)$ denote the cumulative distribution function and quantile function of the univariate Student's t-distribution with ν degrees of freedom, and $t_{\nu,\rho}(\cdot, \cdot)$ denotes the corresponding bivariate Student's t-distribution with correlation ρ. The parameter θ controls the strength of dependence in the Archimedean copulas, with $\theta > 0$ for the Clayton family and $\theta \geq 1$ for the Gumbel family.

Table 1: Copula families and their rotated versions used in the vine model.

Family	Copula formula	Parameter(s)	Tail Dependence
Gaussian	$\Phi_\rho\big(\Phi^{-1}(u),\, \Phi^{-1}(v)\big)$	$\rho \in (-1, 1)$	None
Student-t	$t_{\nu,\rho}\big(t_\nu^{-1}(u),\, t_\nu^{-1}(v)\big)$	$\rho \in (-1, 1)$, $\nu > 0$	Upper & Lower
Clayton	$(u^{-\theta} + v^{-\theta} - 1)^{-1/\theta}$	$\theta > 0$	Lower
Clayton 90°	$v - ((1-u)^{-\theta} + v^{-\theta} - 1)^{-1/\theta}$	$\theta > 0$	Negative
Clayton 180°	$u + v - 1 + ((1-u)^{-\theta} + (1-v)^{-\theta} - 1)^{-1/\theta}$	$\theta > 0$	Upper
Clayton 270°	$u - (u^{-\theta} + (1-v)^{-\theta} - 1)^{-1/\theta}$	$\theta > 0$	Negative
Gumbel	$\exp\Big\{-\big[(-\ln u)^\theta + (-\ln v)^\theta\big]^{1/\theta}\Big\}$	$\theta \geq 1$	Upper
Gumbel 90°	$v - \exp\Big\{-\big[(-\ln(1-u))^\theta + (-\ln v)^\theta\big]^{1/\theta}\Big\}$	$\theta \geq 1$	Negative
Gumbel 180°	$u + v - 1 + \exp\Big\{-\big[(-\ln(1-u))^\theta + (-\ln(1-v))^\theta\big]^{1/\theta}\Big\}$	$\theta \geq 1$	Lower
Gumbel 270°	$u - \exp\Big\{-\big[(-\ln u)^\theta + (-\ln(1-v))^\theta\big]^{1/\theta}\Big\}$	$\theta \geq 1$	Negative

2.6 Value at risk and expected shortfall calculation

2.6.1 VaR for copula models

Let d denote the number of assets in the portfolio and let $\mathbf{w} = (w_1, \ldots, w_d)^\top$ be the vector of portfolio weights, where $w_j = 1/d$ for all $j = 1, \ldots, d$. Let $t + 1$ denote the 1-day-ahead forecast horizon and let $\widehat{\sigma}_{j,t+1}$ be the conditional volatility of asset j at horizon $t + 1$.

Let $\mathbf{Z} = (\widehat{Z_1}, \ldots, \widehat{Z_d})^\top$, denote standardized residuals of length 10000, simulated from the fitted vine copula model with skewed Student's t-marginals. The simulated return of asset j at horizon $t + 1$ is given by

$$\widehat{R}_{j,t+1} = \widehat{\sigma}_{j,t+1}\widehat{Z_j}, \qquad j = 1, \ldots, d. \tag{13}$$

The corresponding simulated portfolio return is

$$\widehat{\boldsymbol{R}}_{\boldsymbol{t+1}} = \sum_{j=1}^{d} w_j \widehat{R}_{j,t+1} = \sum_{j=1}^{d} w_j \widehat{\sigma}_{j,t+1} Z_j, \tag{14}$$

For a confidence level $\alpha \in (0, 1)$, the VaR of the portfolio 1 day-ahead is defined as the lower α-quantile of the portfolio return distribution:

$$\mathrm{VaR}_{\alpha,t+1} = \inf\left\{x \in \mathbb{R} : \mathbb{P}(\widehat{\boldsymbol{R}}_{\boldsymbol{t+1}} \leq x) \geq \alpha\right\}. \tag{15}$$

For backtesting purposes, a VaR exceedance (hit) indicator is defined as

$$\mathbb{I}_{t+1}(\alpha) = \mathbf{1}\left\{\boldsymbol{R_{t+1}}^{\text{real}} < \text{VaR}_{\alpha,t+1}\right\}, \tag{16}$$

where $\boldsymbol{R_{t+1}}^{\text{real}}$ denotes the realized equally weighted portfolio return at time $t+1$.

2.6.2 Expected shortfall

The Expected Shortfall (ES) at level α and horizon h is defined as the expected portfolio simulated return conditional on simulated returns falling below the VaR threshold:

$$\text{ES}_{\alpha,t+1} = \mathbb{E}\left[\widehat{\boldsymbol{R}}_{\boldsymbol{t+1}} \mid \widehat{\boldsymbol{R}}_{\boldsymbol{t+1}} \leq \text{VaR}_{\alpha,t+1}\right]. \tag{17}$$

2.7 Moving window approach

For each asset, a fixed-size rolling window of 1000 historical observations is used to estimate the parameters of an ARMA(1,1)–GARCH–type model, where the ARMA component captures conditional mean dynamics [14, 30] with different volatility models specified in sections before. The window rolls forward through time, refitting the model every 10 observations to balance computational efficiency with parameter adaptability. The standardized residuals of each window i and asset j (denoted as $z_{j,t}^{(i)}$) are computed by dividing the mean-adjusted returns by the conditional volatility estimates. The rolling procedure generates one-step-ahead conditional volatility forecasts ($\widehat{\sigma}_{j,t+1}$) for each time point.

The extracted residuals undergo diagnostic testing using Ljung-Box tests for serial correlation, Ljung-Box tests on squared residuals for remaining ARCH effects, and ARCH-LM tests. Only models that pass these diagnostic criteria with 5% significance are retained for further analysis, ensuring that the standardized residuals exhibit the white noise properties required for subsequent copula modelling.

This extraction process provides the essential inputs for the vine copula framework: properly standardized residuals that capture the pure innovations from each marginal model, along with corresponding volatility forecasts needed for risk aggregation and backtesting.

Let

$$\boldsymbol{z}_t^{(i)} = \left(z_{1,t}^{(i)}, z_{2,t}^{(i)}, \ldots, z_{d,t}^{(i)}\right)$$

denote the vector of standardized residuals of volatility model at time t corresponding to a given window.

In the next step, for each rolling window, with window size W, $i = 1, \ldots, T - W$, the joint dependence structure of the residual vector

$$\{\boldsymbol{z}_t\}_{t=i}^{i+W-1}$$

is modelled using a vine copula. Prior to dependence modelling, the marginal distributions of the standardized residuals are estimated parametrically within each rolling window using a skewed Student's t-distribution. The standardized residuals are then transformed to the unit interval via the probability integral transform (PIT):

$$U_{j,t} = F_{\text{skewed-t}}\left(z_{j,t}\right), \quad j = 1, \ldots, d.$$

Based on the resulting multivariate copula model, joint simulations of standardized residuals are generated for each window. These simulated residuals are then rescaled using the corresponding volatility forecasts obtained from the rolling volatility models.

Finally, for each window, the simulated portfolio return distribution is constructed and used to compute one-day-ahead VaR forecasts at the desired confidence levels. The realized portfolio returns are then compared with the corresponding VaR forecasts, allowing for out-of-sample backtesting of the risk model. Additionally, Expected Shortfall is estimated using given VaR.

This moving window approach ensures that both marginal dynamics and dependence structures are allowed to evolve over time, providing a flexible framework for capturing time-varying risk characteristics in multivariate financial portfolios.

2.8 Backtesting value at risk

VaR backtesting evaluates whether the risk model accurately captures extreme losses by comparing predicted VaR levels with realized returns.

2.8.1 Basel traffic light test

The Basel Traffic Light Test evaluates whether the risk model accurately captures extreme losses by comparing predicted VaR levels with realized returns, where model performance is assessed by the number of VaR exceptions and their cumulative binomial probability as formalized in the Basel Traffic Light Test [4, 18].

Table 2: Model evaluation zones based on exceedance probability.

Zone	Condition
Green Zone	$\mathbb{P}(X \leq x) < 0.95$
Yellow Zone	$0.95 \leq \mathbb{P}(X \leq x) < 0.9999$
Red Zone	$\mathbb{P}(X \leq x) \geq 0.9999$

One of the criteria of rejecting the model is when the red colour assigned. Yellow light may indicate potential model problems that warrant further analysis.

2.8.2 Unconditional coverage (Kupiec) test

Let $N = T - W$ be the total number of observations and

$$x = \sum_{t=1}^{N} \mathbb{I}_{t+1}(\alpha)$$

the total number of VaR violations.

The unconditional coverage test examines whether the observed frequency of VaR violations is consistent with the nominal confidence level. A rejection of the null hypothesis indicates systematic underestimation or overestimation of risk [16, 36].

The likelihood ratio test statistic is

$$LR_{\text{POF}} = -2 \ln \left(\frac{(1-\alpha)^{N-x} \alpha^x}{\left(1 - \frac{x}{N}\right)^{N-x} \left(\frac{x}{N}\right)^x} \right),$$

which asymptotically follows a chi-squared distribution with one degree of freedom:

$$LR_{\text{POF}} \sim \chi^2(1).$$

2.8.3 Independence test

Following the likelihood-based framework for testing interval forecasts introduced by Christoffersen [16], the independence of VaR violations can be examined using a transition matrix of exceedance indicators.

Let n_{ij} denote the number of transitions from state i at time $t-1$ to state j at time t, where $i, j \in \{0, 1\}$. The transition probabilities are defined as

$$\pi_{01} = \frac{n_{01}}{n_{00} + n_{01}}, \qquad \pi_{11} = \frac{n_{11}}{n_{10} + n_{11}}.$$

Under the null hypothesis of independence, the likelihood function is

$$L_0 = (1-\pi)^{n_{00}+n_{10}} \pi^{n_{01}+n_{11}}, \qquad \pi = \frac{n_{01} + n_{11}}{T}.$$

The unrestricted likelihood is

$$L_1 = (1-\pi_{01})^{n_{00}} \pi_{01}^{n_{01}} (1-\pi_{11})^{n_{10}} \pi_{11}^{n_{11}}.$$

The independence test statistic is

$$LR_{\text{IND}} = -2 \ln \left(\frac{L_0}{L_1} \right) \sim \chi^2(1).$$

2.8.4 Conditional coverage (CC) test

The conditional coverage test combines the unconditional coverage and independence tests:

$$LR_{\text{CC}} = LR_{\text{POF}} + LR_{\text{IND}} \sim \chi^2(2).$$

The conditional coverage test checks whether the number of violations is correct and whether violations occur independently. This joint likelihood ratio test of coverage and independence was developed by Christoffersen [16]. Passing this test indicates that the VaR model performs well overall.

2.9 Backtesting expected shortfall

For ES backtesting we consider the Exceedance Residual (ER), Conditional Calibration (CCL) and ES Regression (ESR), briefly described in Sections 2.9.1–2.9.3 Let $\{\boldsymbol{R_t}^{real}\}_{t=1}^{T}$ denote a sequence of portfolio returns and let $q_{t+1}(\alpha)$ and $e_{t+1}(\alpha)$ be the corresponding one-step-ahead VaR and ES forecasts at level $\alpha \in (0, 1)$.

2.9.1 Exceedance residual (ER) backtest

Following McNeil and Frey [40], we define the exceedance residual as the difference between the realized return and the Expected Shortfall forecast, standardized by the conditional standard deviation $\hat{\sigma}_{t+1}$:

$$ER_{t+1} = \frac{e_{t+1}(\alpha) - \boldsymbol{R_{t+1}}}{\hat{\sigma}_{t+1}} \mathbb{I}_{t+1}(\alpha), \tag{18}$$

where $\mathbb{I}_{t+1}(\alpha) = I\{\boldsymbol{R_{t+1}} \leq q_{t+1}(\alpha)\}$ is the indicator function for VaR violations.

The null hypothesis of a correct Expected Shortfall specification is that these residuals have a conditional mean of zero:

$$H_0 : \quad \mathbb{E}[ER_{t+1}] = 0. \tag{19}$$

2.9.2 Conditional calibration (CCL) backtest

The CCL backtest of Nolde and Ziegel [50] is based on the joint identification function for VaR and ES,

$$V_{t+1}(q_{t+1}, e_{t+1}, \widehat{\boldsymbol{R}}_{\boldsymbol{t+1}}) = \begin{pmatrix} \mathbb{I}\{\widehat{\boldsymbol{R}}_{\boldsymbol{t+1}} \leq q_{t+1}\} - \alpha \\ e_{t+1} - q_{t+1} + \dfrac{1}{\alpha}(q_{t+1} - \widehat{\boldsymbol{R}}_{\boldsymbol{t+1}})\mathbb{I}\{\widehat{\boldsymbol{R}}_{\boldsymbol{t+1}} \leq q_{t+1}\} \end{pmatrix}. \tag{20}$$

Let Z_t denote a vector of instruments measurable with respect to the information set $\mathcal{F}_t$. The null hypothesis of conditional calibration is

$$H_0 : \quad \mathbb{E}[Z_t \otimes V_{t+1}(q_{t+1}, e_{t+1}, \boldsymbol{R_{t+1}})] = 0, \tag{21}$$

where $\otimes$ denotes the Kronecker product.

2.9.3 ES regression (ESR) backtest

The ESR backtest of Bayer and Dimitriadis [6] utilizes a joint Mincer-Zarnowitz regression framework. Since ES is not evaluated independently stand-alone, the test is based on a joint regression model for the VaR and the ES.

In the Strict ESR specification, which only requires ES forecasts as input variables, we estimate the following joint system for portfolio returns $\widehat{\boldsymbol{R}}_{\boldsymbol{t+1}}$ and ES forecasts $e_{t+1}(\alpha)$:

$$\begin{aligned} \widehat{\boldsymbol{R}}_{\boldsymbol{t+1}} &= \alpha_1 + \alpha_2 e_{t+1}(\alpha) + u^q_{t+1}, \\ \widehat{\boldsymbol{R}}_{\boldsymbol{t+1}} &= \beta_1 + \beta_2 e_{t+1}(\alpha) + u^e_{t+1}, \end{aligned} \tag{22}$$

where (α_1, α_2) are the auxiliary VaR parameters, (β_1, β_2) are the ES-specific parameters and u is error term. The null hypothesis of a correctly specified Expected Shortfall is defined by the ES-specific regression coefficients:

$$H_0 : \quad \beta_1 = 0 \quad \text{and} \quad \beta_2 = 1. \tag{23}$$

Under H_0, the ES forecasts are correctly specified such that

$$e_{t+1}(\alpha) = \mathbb{E}[\widehat{\boldsymbol{R}}_{\boldsymbol{t+1}} | \widehat{\boldsymbol{R}}_{\boldsymbol{t+1}} \leq q_{t+1}].$$

3 Data

In this section we present daily asset returns used for the analysis, obtained from Yahoo Finance and EU ETS. The sample covers the period from 2018 November 27 to 2025 November 21, all assets in portfolio are chosen to be equally weighted.

The iShares USD Green Bond ETF (BGRN) is included to represent green bonds, whose funds are used exclusively to finance climate-related and other environmental projects. Clean energy equities are proxied by the iShares Global Clean Energy ETF (ICLN), which reflects the performance of firms engaged in renewable energy production and related technologies, while the Invesco Solar ETF (TAN) provides more targeted exposure to the solar energy sector. In addition, EU Emissions Allowances (EUA) are incorporated to represent ETS.

To capture the interaction between green assets and the broader economic and financial environment, several conventional market indicators are included. The S&P 500 index (GSPC) represents global equity market conditions and overall investor sentiment.

Gold futures (GCF) are employed as a traditional safe-haven asset, often associated with periods of heightened uncertainty and inflationary pressure, while copper futures (HGF) serve as a proxy for global industrial activity and economic growth, reflecting demand conditions in manufacturing and energy infrastructure. Natural gas futures (TTFF) are included to represent energy market dynamics and supply-side shocks, particularly relevant during periods of energy market stress.

Finally, we choose Cardano (ADA) as a proxy for clean cryptocurrencies, for being one of the largest in its class. Also, we consider Bitcoin (BTC) to oppose ADA for being the largest by market capitalisation.

4 Main results

For each asset an adequate univariate return model has been fitted. Based on the outcomes of the Basel Traffic Light Test, the unconditional coverage, independence and conditional coverage tests. GJR-GARCH model was best suited for BGRN, GCF, HGF, GSPC, ICLN and TAN assets, while csGARCH was more suitable for EUA, TTFF and ADA assets. For BTC asset the best fit was eGARCH model.

Table 3 shows the number of actual violations for different assets and their corresponding Basel zones. Assets BGRN, HGF, ICLN, TAN, EUA, TTFF, ADA and BTC have relatively low violations and fall within the Green Basel zone, suggesting that the predicted VaR aligns well with actual losses. In contrast, GCF and GSPC have higher violations and are classified in the Yellow Basel zone, signaling moderate risk and the need for closer monitoring.

Table 3: Basel 99% VaR Backtesting Results.

Asset	Backtesting days	Violations	Basel zone	Volatility model
BGRN	757	15	Green	GJR-GARCH
GCF	1237	28	Yellow	GJR-GARCH
HGF	1238	24	Green	GJR-GARCH
GSPC	1236	27	Yellow	GJR-GARCH
ICLN	1236	15	Green	GJR-GARCH
TAN	1236	21	Green	GJR-GARCH
EUA	1287	24	Green	csGARCH
TTFF	1035	12	Green	csGARCH
ADA-USD	1938	28	Green	csGARCH
BTC-USD	2249	21	Green	eGARCH

Table 4 presents the results of backtesting for Value-at-Risk (VaR) models across the assets. We present the results of Unconditional Coverage, Independence, and Conditional Coverage tests. Most assets fail to reject the null hypothesis with 5% significance. For these assets, the models predict VaR adequately, the number of exceedances matches the theoretical expectation, and they are spread out independently over time. However, for EUA, GCF and GSPC the results suggest potential inadequacy in captur-

Table 4: Conditional Coverage, Independence, and Unconditional Coverage Test Results.

	Conditional Coverage Test		Independence Test		Unconditional Coverage Test		
Asset	VaR 95%	VaR 99%	VaR 95%	VaR 99%	VaR 95%	VaR 99%	Volatility model
ADA	1.00000	0.71600	0.79600	0.85600	0.96700	0.92100	csGARCH
BGRN	0.72229	**0.01668**	0.06958	-	0.18094	-	GJR-GARCH
BTC	0.84100	0.87400	0.19600	0.06100	0.42600	0.17000	eGARCH
EUA	0.07691	**0.00537**	0.06238	**0.00869**	**0.03685**	**0.00066**	csGARCH
ICLN	0.61645	0.46525	0.86267	-	0.86901	-	GJR-GARCH
TAN	0.23960	**0.02472**	0.27600	-	0.27670	-	GJR-GARCH
GCF	0.78027	**0.00013**	0.69936	0.15706	0.89272	**0.00024**	GJR-GARCH
HGF	0.88625	**0.00328**	0.65271	0.48632	0.89451	**0.01041**	GJR-GARCH
GSPC	**0.02281**	**0.00030**	0.93145	0.61863	0.07462	**0.00127**	GJR-GARCH
TTFF	0.32526	0.61515	1.00000	0.12528	1.00000	0.27215	csGARCH

ing extreme tail risk. In some cases, test statistics are not reported (indicated by "-"). This occurs when the number of VaR exceedances is either zero or equal to the expected number under the nominal coverage level, which prevents the computation of likelihood-based backtesting statistics. In particular, the Independence and Conditional Coverage tests require a minimum number of violations to estimate transition probabilities between exceedance states. When this condition is not satisfied, the corresponding test is not well-defined and therefore omitted.

After selecting optimal univariate models, we proceed with constructing a portfolio and fitting appropriate Vine Copula models for the univariate residuals. By comparing several alternative portfolio structures and performing comprehensive backtesting for each, we conclude with a final model that excludes both cryptocurrencies. Backtesting indicated that Cardano (ADA) had a significant negative impact on model accuracy, its inclusion caused the violation rate to increase drastically and introduced significant dependence between violations. Furthermore, after excluding ADA and remaining with BTC, the results continued to show dependent violations, suggesting that the volatility of the crypto market is incompatible with the chosen portfolio. The 8-asset R-vine and C-vine models, consisting of traditional commodities, equities, and green energy indices, showed robust results for the 1-day-ahead horizon. As shown in Table 5, at both 1% and 5% confidence levels, the Kupiec test p-values exceed 0.05, meaning statistically significant actual violations rate alignment with expected rate. Independence and Conditional Coverage tests confirm that violations are not clustered, meaning models pass all three fundamental VaR backtesting criteria. Additionally, both vine models fall within the "Green" zone of the Basel traffic light system. Comparing the two vine structures in Table 6, it is seen that the R-vine slightly outperforms the C-vine, as demonstrated by its lower Average AIC (-2890.044) and BIC (-2801.852). Results in Table 7 illustrate that both models remain valid at the 99% confidence level (p-values of all tests are greater than 0.05). However, at the 95% level, the models show marginal performance (some p-values being less than 0.05), suggesting that while the models accurately predict VaR, they may struggle to estimate reliable losses having a breach in

VaR. Since the average AIC and BIC are lower for the R-vine, and this structure exhibits more flexibility, in the following analysis we focus on describing and interpreting results only for the R-vine model. The corresponding 1% and 5% VaR and ES estimates are illustrated in Figures 5 and 6.

Table 5: Backtesting results comparison. **Notation:** ER – expected rate of violations, AR – actual rate of violations, POF – p-value of proportion of failures (Kupiec) test, IND – p-value of independence test, CC – p-value of conditional coverage test.

Model	Horizon	Confidence	ER	AR	POF	IND	CC	Basel traffic light
R-vine	1d	99%	0.010	0.015	0.346	0.121	0.192	Green
	1d	95%	0.050	0.056	0.464	0.096	0.192	Green
C-vine	1d	99%	0.010	0.015	0.203	0.151	0.159	Green
	1d	95%	0.050	0.055	0.569	0.079	0.182	Green

Table 6: Average information criteria of both models.

Model	Average AIC	Average BIC
R-vine	-2890.044	-2801.852
C-vine	-2886.251	-2795.934

Table 7: Expected Shortfall backtesting results. **Notation:** ER – Exceedance Residual test, CCL – Conditional Calibration test, ESR – Expected Shortfall Regression test.

Model	Confidence	ER p-value	CCL p-value	ESR p-value
R-vine	99%	0.100	0.170	0.267
	95%	0.069	0.171	0.048
C-vine	99%	0.123	0.196	0.247
	95%	0.048	0.129	0.037

Table 8 describes the learned unconditional dependence structure throughout the rolling window exercise, which reveals a distinct hierarchy characterized by clear thematic clustering and asymmetric tail risks. The strongest and the most robust dependence is observed within the clean energy sector itself, with the ICLN-TAN pair exhibiting exceptionally high mean Kendall's τ of 0.76, and symmetric tail dependence. This "lockstep" behaviour indicates that despite sub-sector differences, these assets respond almost identically to systemic shocks, offering little diversification benefit against one another.

Furthermore, the observed results challenge the decoupling hypothesis regarding the broader equity market. Clean energy assets maintain a moderate-to-strong integration

Table 8: This table presents descriptive statistics for the unconditional dependence structure between asset pairs, averaged across the full rolling window estimation period. **Notation:** $\bar{\tau}$ denotes the mean unconditional Kendall's rank correlation coefficient; sd(τ), min, and max represent the standard deviation, minimum, and maximum values of τ, respectively; Q_2 and Q_3 correspond to the median and 75th percentile of the correlation distribution. The columns $\bar{\lambda}_L$ and $\bar{\lambda}_U$ report the mean empirical lower and upper tail dependence coefficients, respectively, quantifying the probability of simultaneous extreme negative or positive returns.

Assets		$\bar{\tau}$	sd(τ)	min $\bar{\tau}$	max $\bar{\tau}$	$\bar{\tau}(Q_2)$	$\bar{\tau}(Q_3)$	$\bar{\lambda}_L$	$\bar{\lambda}_U$
ICLN	TAN	0.76	0.02	0.70	0.80	0.75	0.78	0.74	0.74
GSPC	ICLN	0.42	0.02	0.35	0.47	0.40	0.43	0.38	0.37
GSPC	TAN	0.36	0.02	0.31	0.41	0.35	0.37	0.32	0.33
BGRN	GCF	0.20	0.02	0.13	0.25	0.19	0.21	0.19	0.19
GCF	HGF	0.16	0.02	0.09	0.22	0.14	0.17	0.23	0.11
HGF	GSPC	0.15	0.05	0.03	0.26	0.11	0.19	0.13	0.12
BGRN	ICLN	0.14	0.06	0.03	0.24	0.08	0.19	0.15	0.15
HGF	ICLN	0.13	0.04	0.02	0.20	0.09	0.16	0.13	0.10
BGRN	TAN	0.12	0.05	0.02	0.22	0.07	0.16	0.14	0.13
BGRN	GSPC	0.11	0.05	0.00	0.20	0.07	0.15	0.12	0.13
HGF	TAN	0.11	0.04	0.01	0.19	0.08	0.14	0.12	0.09
GCF	ICLN	0.11	0.03	0.04	0.18	0.09	0.13	0.11	0.13
GCF	TAN	0.08	0.02	0.01	0.14	0.06	0.10	0.10	0.12

with the S&P 500, with mean τ ranging from 0.36 to 0.42. Notably, the estimated Vine Tree structures position ICLN as the central bridge connecting the broader equity market to the specialized green sector (TAN). This suggests that clean energy assets currently are still sensitive to general market sentiment, rather than act as isolated alternative asset class. Given the reliance of green innovation on technological breakthroughs, it is not surprising that these assets exhibit the volatility profiles typical of the technology sector. However, partial decoupling may emerge as the industry matures from a speculative growth phase into established critical infrastructure, governed by regulatory and demand drivers.

Furthermore, we observe a pronounced asymmetry in the commodity-green nexus. While Gold (GCF) and Copper (HGF) display a weak average correlation ($\bar{\tau} = 0.16$), their tail behaviour reveals a hidden systemic risk. The probability of joint crashes ($\bar{\lambda}_L = 0.23$) is more than double the probability of joint growth ($\bar{\lambda}_U = 0.11$). This "panic coupling" implies that industrial metals and safe-haven assets, which typically follow different cycles [23], tend to re-couple dangerously during severe market downturns, likely amplifying liquidity stress for green technologies reliant on these raw materials. Thus Gold cannot be confidently relied upon as a perfect hedge for green technology during systemic crises.

Note, that in contrast to the equity-heavy clean energy sector, Green Bonds (BGRN) emerge as the most effective diversifier. The Table 8 highlights consistently low correlations with both the S&P 500 ($\bar{\tau} = 0.11$) and clean energy equities ($\bar{\tau} = 0.14$). Interestingly, BGRN shows a stronger relative linkage to Gold ($\bar{\tau} = 0.2$), suggesting its

performance is driven more by interest rate and safe-haven flows than by the ”risk-on” technology cluster. This validates the role of Green Bonds as a portfolio stabilizer.

Moving beyond the static averages, the dynamic Vine Copula analysis demonstrates a profound structural shift in how green markets transmit risk. As illustrated by Figure 2, ICLN acts as the dominant hub for the majority of the sample, reinforcing its role as the central transmitter of shocks in the green economy. In the beginning of the sample, potentially strongly affected by the 2020–2022 volatility, the market dynamics shift dramatically over time, but in the latter half of the sample the network topology locks into a stable R-Vine structure. When ICLN moves, it pulls the entire network – S&P 500, Solar stocks, and Green Bonds. This can be observed in Figure 2, that shows persistently high and stable dependency between ICLN and its satellites.

However, a secondary, unstable hub emerges around Gold. Our analysis indicates that Gold's ability to act as a central node is fragile and directly linked to the Carbon market (EUA). The presence and signal strength of Carbon allowances acts as a switch, i.e., only when EUA signals are active in the structure does Gold successfully consolidate the commodity cluster. However, as seen by Figure 2, this relationship is volatile. The connection between the Gold and EUA ”flickers”, leading to periods where the commodity hub disintegrates. Notably, during these low-magnitude periods the conservative independence tests often fail to reject the null, rendering some dependency estimates statistically indistinguishable from zero. We deem that this statistical invisibility does not imply a lack of economical linkage, but rather the existence of a mixture of opposing forces, pulling the market in different directions. On a pro-cyclical movement, the industrial demand pulls carbon prices up when the economy (along with the commodities) are growing. On a counter-cyclical aspect, the regulatory intervention and ”green hedging” demand can push prices up even when the broad market falls. The cancelling out of these vectors may result in a near-zero net correlation in certain periods. This erratic behaviour highlights the lack of maturity of the investor base and sentiment surrounding regulatory assets, as the market has not yet settled on a consistent pricing model for carbon risk.

Importantly, we observe a distinct regime change around the rolling window corresponding to June 2024. Note, that the observed date is lagging due to the large training window selected for the rolling window experiment. However, this pivot point marks the interesting transition of the green market from a previous ”crisis response” regime to a ”structural integration” regime. Judging from the stress index, presented by Figure 4, around that point a peak was reached, and then sharply declined. In the context of post-pandemic volatility and the 2022 energy crisis, the observed decline suggests that the recent market stability in 2023–2024 has began to dilute the impact of the earlier shocks. As the immediate correlation between fossil fuels and green assets weakens in the recent data, the network decouples from the geopolitical conflict signals. Paradoxically, while the average correlation dropped, the structural risk increased, at which the network confidently shifts to a centralised hub structure (R-Vines). The structural hardening is confirmed by the average path length metric, see Figure 1, which drops significantly in the post-June 2024 period. In Network theory, a shorter path length implies a faster transmission mechanism of the shocks in the network. Thus, while the market is less stressed on the average, it has become more efficient at transmitting shocks. A fail-

ure in the central green hub (through ICLN) now propagates to the periphery (through Bonds and Commodities) more rapidly than it did during the early crisis years.

Fig. 1 Average path length in the estimated vine structure at ever point of the rolling window experiment.

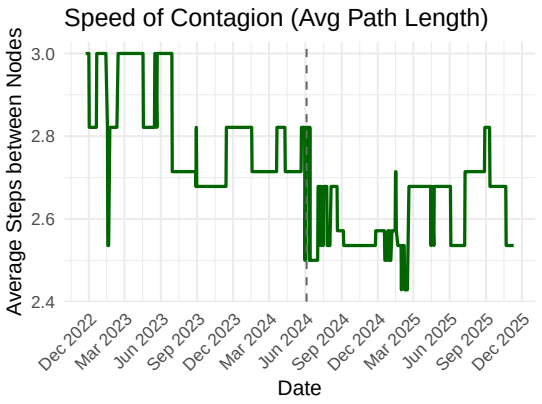

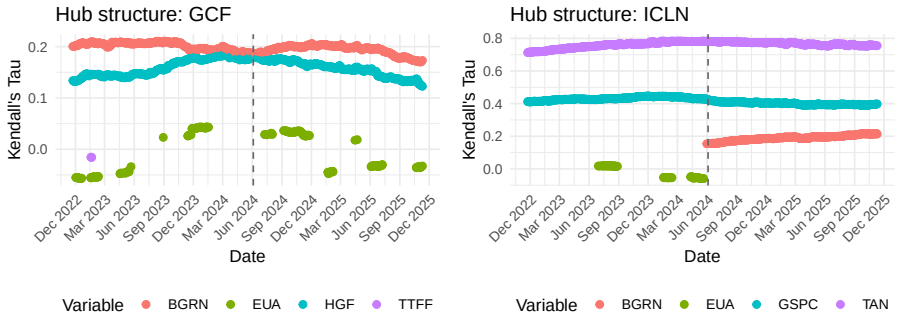

Fig. 2: The figure demonstrates the Kendall's Tau values around two hubs throughout the rolling window experiment. Namely, the GCF **(left)** and ICLN **(right)**. The colors denote different variables, while the black vertical line denotes the observed structural shift around June 2024.

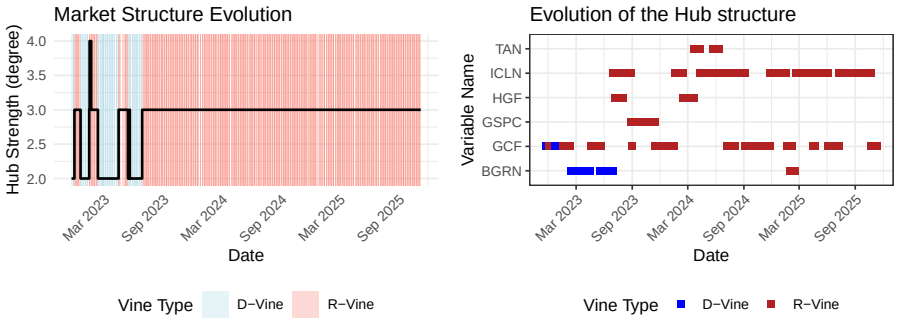

Fig. 3: The topological evolution of the market network, showing the unstable switch from a D-Vine structure into R-Vine structures **(left)**, when the hubs start to consistently appear. In order to better understand the dynamic changes, on the **right** graph we present the evolving "hubs".

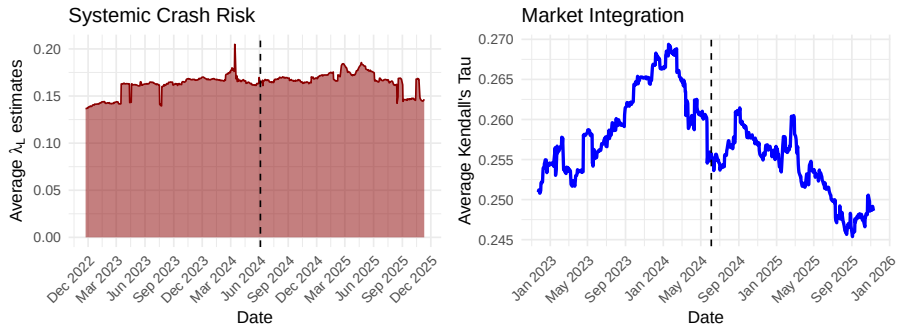

Fig. 4: On the **left** graph we demonstrate the average λ_L values of the whole vine copula structure and it's dynamics throughout the rolling window experiments. Similarly, on the **right** graph we present the average Kendall's Tau values. In both cases the black vertical line denotes the observed structural shift around June 2024.

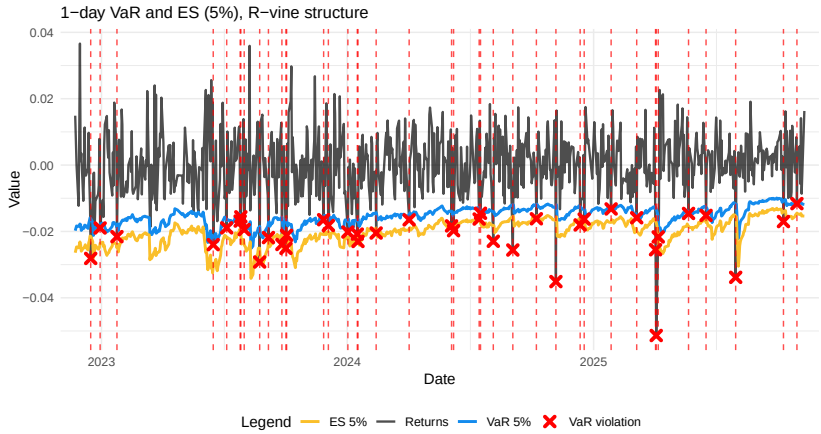

Fig. 6: 1-day VaR and ES (5%) of R-vine structure.

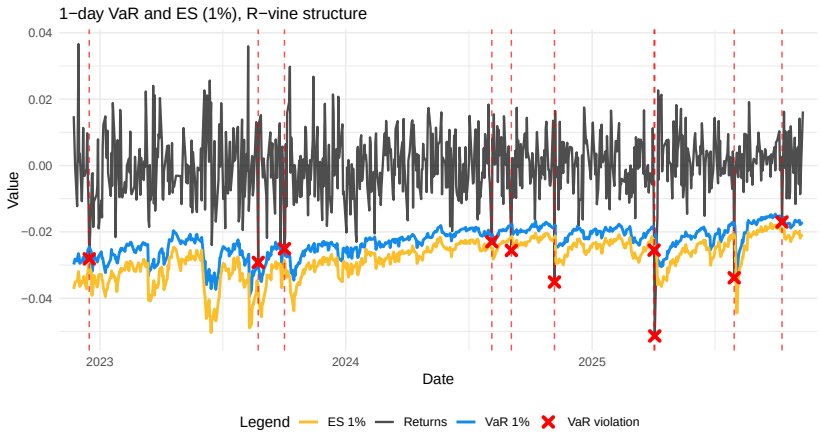

Fig. 5: 1-day VaR and ES (1%) of R-vine structure

Conclusions

In this Chapter, we model the risk dynamics and dependence structure of a portfolio composed of green financial assets, traditional commodities, and broad market indices. By employing a rolling-window ARMA-GARCH-Vine Copula framework, we identified the specific transmission channels of financial stress and evaluated the diversification potential of the green economy.

The univariate analysis confirms that green finance is not a monolithic asset class. We found that sustainable instruments exhibit highly distinct risk behaviours, ranging from the stable, mature profiles of Green Bonds, to the complex, long-memory volatility of Carbon allowances. Our risk modelling demanded the exclusion of clean cryptocurrencies from the final portfolio. Both Cardano and Bitcoin exhibited extreme volatility and dependent VaR violations.

The multivariate dependence analysis shows that the green assets are moving from their earlier speculative phase and is becoming a more accepted part of the global financial system. Our results reject the ”decoupling hypothesis” as a universal characteristic of green finance. Instead, we observe a clear division. Clean Energy equities (ICLN) and Solar stocks (TAN) move in lockstep and maintain moderate integration with the S&P 500. With the Vine methodology the Clean Energy ETF is identified as a central ”risk hub”, effectively transmitting broad market shocks into the specialized green sector. In contrast, Green Bonds have successfully decoupled, behaving more like stabilizing fixed-income instruments than speculative technology assets, validating their role as effective portfolio diversifiers.

The analysis of traditional commodities reveals hidden tail risks. While Gold and Copper display a weak average correlation, we observe strong asymmetric tail dependence. The probability of simultaneous extreme losses is more than double the probability of simultaneous gains. Such ”panic coupling” suggests that during the severe market

downturns, industrial and safe-haven commodities synchronize, significantly reducing the hedging efficiency of Gold when it is most needed. Furthermore, the relationship between Gold and Carbon allowances was found to be unstable, too weak to form a consistent commodity hub.

The dynamic rolling-window analysis identified a structural shift in the market, observable in our results since around June 2024. The Vine topology transitioned from an unstable sequential D-Vine structure to a centralised R-Vine structure dominated by Clean Energy ETF. Coinciding with this shift, the average path length of the network dropped significantly, indicating that the transmission of shocks has become more efficient. While the overall market volatility has declined since the 2022 energy crisis, the market structure has become observably more centralised. The results suggest that shocks to the clean energy hub are likely to spread to other assets more rapidly than in previous regimes.

These findings have several implications for investors. Green Bonds stand out as an effective hedge, maintaining low and stable correlations with both the broader equity market and clean energy assets. Gold, despite its safe-haven reputation, does not consistently provide protection during systemic downturns, as it tends to move together with industrial metals (proxied by copper) during market stress. Also, the expanding importance of ICLN raises caution, as shocks to this single ETF may now spread more quickly across the green asset market. Meanwhile, carbon credits should be treated carefully, given their unstable behaviour and sensitivity to regulatory changes.

Finally, the results highlight several directions for future research. First, the growing centralization of the green financial network around Clean Energy ETFs suggests the need to study the velocity of shock transmission. Future studies should consider additional connectedness measures, such as Diebold-Yilmaz spillover indices or Causal Vine copulas, potentially across a wider variety of assets, including upstream supply chain equities and sovereign green bonds to more accurately map the evolving topology of sustainable finance.

Furthermore, special attention should be paid to validating the drivers of the observed structural shift in dependence. While this study posits that the shift post-2024 stems from the ”washing-out” of post-pandemic-era volatility, future work should employ formal structural break tests to pinpoint the exact timing of the decoupling without the inherent lag effects due to the rolling window estimation.

Finally, the exclusion of cryptocurrencies and the backtesting challenges associated with certain commodities suggest that standard volatility models are insufficient for the most volatile assets. Future research could employ Markov-Switching GARCH or Extreme Value Theory to explicitly capture regime-dependent tail risks. Such methodological advancements would potentially allow for the safe inclusion of high-volatility instruments, enabling the construction of larger, more resilient portfolios than the one considered in this work.

References

1. Aas, K., Czado, C., Frigessi, A., & Bakken, H. (2009). Pair-copula constructions of multiple dependence. *Insurance: Mathematics and Economics*, *44*(2), 182–198. https://doi.org/10.1016/j.insmatheco.2007.11.001
2. Aparicio, F. M., & Estrada, J. (2001). Empirical distributions of stock returns: European securities markets, 1990-95. *The European Journal of Finance*, *7*(1), 1–21. https://doi.org/10.1080/13518470122131
3. Arif, M., Naeem, M. A., Farid, S., Nepal, R., & Jamasb, T. (2022). Diversifier or more? Hedge and safe haven properties of green bonds during COVID-19. *Energy Policy*, *168*, Article 113102. https://doi.org/10.1016/j.enpol.2022.113102
4. Basel Committee on Banking Supervision. (1996). *Supervisory framework for the use of backtesting in conjunction with the internal models approach to market risk capital requirements* (Tech. Rep.). Bank for International Settlements.
5. Baur, D. G., & McDermott, T. K. (2010). Is gold a safe haven? International evidence. *Journal of Banking & Finance*, *34*(8), 1886–1898. https://doi.org/10.1016/j.jbankfin.2009.12.008
6. Bayer, S., & Dimitriadis, T. (2020). Regression-based expected shortfall backtesting. *Journal of Financial Econometrics*, *20*(3), 437–471. https://doi.org/10.1093/jjfinec/nbaa013
7. Becker, M. G., Martin, F., & Walter, A. (2022). The power of ESG transparency: The effect of the new SFDR sustainability labels on mutual funds and individual investors. *Finance Research Letters*, *47*, Article 102708. https://doi.org/10.1016/j.frl.2022.102708
8. Bedford, T., & Cooke, R. M. (2002). Vines—A new graphical model for dependent random variables. *The Annals of Statistics*, *30*(4), 1031–1068. https://doi.org/10.1214/aos/1031689016
9. Ben Ameur, H., Ftiti, Z., Louhichi, W., & Yousfi, M. (2024). Do green investments improve portfolio diversification? Evidence from mean conditional value-at-risk optimization. *International Review of Financial Analysis*, *94*, Article 103255. https://doi.org/10.1016/j.irfa.2024.103255
10. Bhutta, U. S., Tariq, A., Farrukh, M., Raza, A., & Iqbal, M. K. (2022). Green bonds for sustainable development: Review of literature on development and impact of green bonds. *Technological Forecasting and Social Change*, *175*, Article 121378. https://doi.org/10.1016/j.techfore.2021.121378
11. Bollerslev, T. (1987). A conditionally heteroskedastic time series model for speculative prices and rates of return. *The Review of Economics and Statistics*, *69*(3), 542–547. https://doi.org/10.2307/1925546
12. Bollerslev, T. (1986). Generalized autoregressive conditional heteroskedasticity. *Journal of Econometrics*, *31*(3), 307–327. https://doi.org/10.1016/0304-4076(86)90063-1
13. Cepni, O., Demirer, R., & Rognone, L. (2022). Hedging climate risks with green assets. *Economics Letters*, *212*, Article 110312. https://doi.org/10.1016/j.econlet.2022.110312
14. Chaiyawat, T., & Guayjarernpanishk, P. (2025). Enhancing insurer portfolio resilience and capital efficiency with green bonds: A framework combining dynamic R-vine copulas and tail-risk modeling. *Risks*, *13*(9), Article 163. https://doi.org/10.3390/risks13090163
15. Cherubini, U., Mulinacci, S., Gobbi, F., & Romagnoli, S. (2011). *Dynamic copula methods in finance*. John Wiley & Sons.
16. Christoffersen, P. F. (1998). Evaluating interval forecasts. *International Economic Review*, *39*(4), 841–862. https://doi.org/10.2307/2527341
17. Climate Bonds Initiative. (2024). *Green bond dataset methodology* (Tech. Rep.). Climate Bonds Initiative.
18. Costanzino, N., & Curran, M. (2018). A simple traffic light approach to backtesting expected shortfall. *Risks*, *6*(1), Article 2. https://doi.org/10.3390/risks6010002
19. de Freitas Netto, S. V., Sobral, M. F. F., Ribeiro, A. R. B., & Soares, G. R. L. (2020). Concepts and forms of greenwashing: A systematic review. *Environmental Sciences Europe*, *32*, Article 19. https://doi.org/10.1186/s12302-020-0300-3
20. Demiralay, S., Gencer, H. G., & Bayraci, S. (2024). Time-scale behaviour of co-movements between renewable energy stocks and other financial assets. In *Transition to the circular economy model: The case of Turkey* (pp. 105–132). Springer. https://doi.org/10.1007/978-3-031-43283-5_6

21. Engle, R. (2002). Dynamic conditional correlation: A simple class of multivariate generalized autoregressive conditional heteroskedasticity models. *Journal of Business & Economic Statistics*, *20*(3), 339–350. https://doi.org/10.1198/073500102288618487
22. Engle, R. F., & Lee, G. G. J. (1999). A long-run and short-run component. In *Cointegration, causality, and forecasting* (p. 475). Oxford University Press.
23. Erb, C. B., & Harvey, C. R. (2006). The strategic and tactical value of commodity futures. *Financial Analysts Journal*, *62*(2), 69–97. https://doi.org/10.2469/faj.v62.n2.4083
24. Glosten, L. R., Jagannathan, R., & Runkle, D. E. (1993). On the relation between the expected value and the volatility of the nominal excess return on stocks. *The Journal of Finance*, *48*(5), 1779–1801. https://doi.org/10.1111/j.1540-6261.1993.tb05128.x
25. Guo, J. (2018). Co-movement of international copper prices, China's economic activity, and stock returns: Structural breaks and volatility dynamics. *Global Finance Journal*, *36*, 62–77. https://doi.org/10.1016/j.gfj.2017.10.002
26. Gursoy, S., Kilic, E., Eksi, I. H., Yudaruddin, R., & Tabash, M. I. (2024). Dynamic volatility interactions between sustainable crypto currencies and green economy indicators. In *2024 International Conference on Sustainable Islamic Business and Finance (SIBF)* (pp. 244–249). IEEE. https://doi.org/10.1109/SIBF61715.2024.10543632
27. Hamilton, J.D. (2009). *Causes and consequences of the oil shock of 2007-08* (Tech. Rep. No. w15002). National Bureau of Economic Research. https://doi.org/10.3386/w15002
28. Hong, Z. (2025). Risks and prevention methods in green finance. *SHS Web of Conferences*, *218*, Article 03018. https://doi.org/10.1051/shsconf/202521803018
29. Hu, Q., & Gu, Y. (2024). Copper economic dynamics: Navigating resource scarcity, price volatility, and green growth. *Resources Policy*, *89*, Article 104462. https://doi.org/10.1016/j.resourpol.2023.104462
30. Ji, H., Wang, H., & Liseo, B. (2018). Portfolio diversification strategy via tail-dependence clustering and ARMA-GARCH vine copula approach. *Australian Economic Papers*, *57*(3), 265–283. https://doi.org/10.1111/1467-8454.12119
31. Joe, H. (1997). *Multivariate models and multivariate dependence concepts*. CRC Press.
32. Joe, H. (2014). *Dependence modeling with copulas*. CRC Press.
33. Karoglou, M. (2010). Breaking down the non-normality of stock returns. *The European Journal of Finance*, *16*(1), 79–95. https://doi.org/10.1080/13518470903036230
34. Kirikkaleli, D. (2021). Analyses of wavelet coherence: Financial risk and economic risk in China. *Journal of Financial Economic Policy*, *13*(5), 587–599. https://doi.org/10.1108/JFEP-03-2020-0061
35. Kristoufek, L. (2015). What are the main drivers of the Bitcoin price? Evidence from wavelet coherence analysis. *PLOS ONE*, *10*(4), Article e0123923. https://doi.org/10.1371/journal.pone.0123923
36. Kupiec, P. H. (1995). Techniques for verifying the accuracy of risk measurement models. *The Journal of Derivatives*, *3*(2), 73–84. https://doi.org/10.3905/jod.1995.407942
37. Lyu, C., & Scholtens, B. (2024). Integration of the international carbon market: A time-varying analysis. *Renewable and Sustainable Energy Reviews*, *191*, Article 114102. https://doi.org/10.1016/j.rser.2023.114102
38. Madani, M. A., & Ftiti, Z. (2022). Is gold a hedge or safe haven against oil and currency market movements? A revisit using multifractal approach. *Annals of Operations Research*, *313*(1), 367–400. https://doi.org/10.1007/s10479-021-04212-3
39. McInerney, C., & Bunn, D. W. (2019). Expansion of the investor base for the energy transition. *Energy Policy*, *129*, 1240–1244. https://doi.org/10.1016/j.enpol.2019.03.037
40. McNeil, A. J., & Frey, R. (2000). Estimation of tail-related risk measures for heteroscedastic financial time series: An extreme value approach. *Journal of Empirical Finance*, *7*(3), 271–300. https://doi.org/10.1016/S0927-5398(00)00012-8
41. Mejdoub, H., & Ghorbel, A. (2018). The dynamic relationship between oil prices and returns on renewable energy companies. *American Journal of Finance and Accounting*, *5*(2), 173–192. https://doi.org/10.1504/AJFA.2018.091321
42. Mensi, W., Belghouthi, H. E., Al-Kharusi, S., & Kang, S. H. (2025). Tail risk contagion and connectedness between clean cryptocurrency, green assets and commodity markets. *International Review of Financial Analysis*, *105*, Article 103823. https://doi.org/10.1016/j.irfa.2025.103823

43. MSCI ESG Research LLC. (2023). *ESG ratings methodology*. MSCI.
44. Naeem, M. A., Adekoya, O. B., & Oliyide, J. A. (2021). Asymmetric spillovers between green bonds and commodities. *Journal of Cleaner Production*, *314*, Article 128100. https://doi.org/10.1016/j.jclepro.2021.128100
45. Naeem, M. A., Bouri, E., Costa, M. D., Naifar, N., & Shahzad, S. J. H. (2021). Energy markets and green bonds: A tail dependence analysis with time-varying optimal copulas and portfolio implications. *Resources Policy*, *74*, Article 102434. https://doi.org/10.1016/j.resourpol.2021.102434
46. Nelsen, R. B. (2006). *An introduction to copulas* (2nd ed.). Springer. https://doi.org/10.1007/0-387-28678-0
47. Nelson, D. B. (1991). Conditional heteroskedasticity in asset returns: A new approach. *Econometrica*, *59*(2), 347–370. https://doi.org/10.2307/2938260
48. Network for Greening the Financial System. (2024). *The green transition and the macroeconomy: A monetary policy perspective* (Tech. Rep.). NGFS.
49. Nguyen, T. T. H., Naeem, M. A., Balli, F., Balli, H. O., & Vo, X. V. (2021). Time-frequency comovement among green bonds, stocks, commodities, clean energy, and conventional bonds. *Finance Research Letters*, *40*, Article 101739. https://doi.org/10.1016/j.frl.2020.101739
50. Nolde, N., & Ziegel, J. F. (2017). Elicitability and backtesting: Perspectives for banking regulation. *The Annals of Applied Statistics*, *11*(4), 1833–1874. https://doi.org/10.1214/17-AOAS1041
51. Omeir, A. K., Štreimikienė, D., & Vasiliauskaitė, D. (2025). Sustainable investments: Assessment of risks. *Journal of Business Economics and Management*, *26*(3), 576–598. https://doi.org/10.3846/jbem.2025.23412
52. Reboredo, J. C. (2015). Is there dependence and systemic risk between oil and renewable energy stock prices? *Energy Economics*, *48*, 32–45. https://doi.org/10.1016/j.eneco.2014.12.009
53. Reboredo, J. C. (2018). Green bond and financial markets: Co-movement, diversification and price spillover effects. *Energy Economics*, *74*, 38–50. https://doi.org/10.1016/j.eneco.2018.05.030
54. Reboredo, J. C., & Ugolini, A. (2020). Price connectedness between green bond and financial markets. *Economic Modelling*, *88*, 25–38. https://doi.org/10.1016/j.econmod.2019.09.004
55. Saeed, T., Bouri, E., & Tran, D. K. (2020). Hedging strategies of green assets against dirty energy assets. *Energies*, *13*(12), Article 3141. https://doi.org/10.3390/en13123141
56. Sharif, A., Brahim, M., Dogan, E., & Tzeremes, P. (2023). Analysis of the spillover effects between green economy, clean and dirty cryptocurrencies. *Energy Economics*, *120*, Article 106606. https://doi.org/10.1016/j.eneco.2023.106606
57. Silvennoinen, A., & Teräsvirta, T. (2009). Multivariate GARCH models. In *Handbook of financial time series* (pp. 201–229). Springer. https://doi.org/10.1007/978-3-540-71297-8_9
58. Sklar, M. (1959). Fonctions de répartition à n dimensions et leurs marges. *Annales de l'ISUP*, *8*(3), 229–231.
59. Su, Y. H., Rizvi, S. K. A., Umar, M., & Chang, H. (2023). Unveiling the relationship between oil and green bonds: Spillover dynamics and implications. *Energy Economics*, *127*, Article 107055. https://doi.org/10.1016/j.eneco.2023.107055
60. Suimon, Y. (2024). Copper as a central commodity in network analysis of price dynamics and its connection to macroeconomic indicators. In *17th International Congress on Advanced Applied Informatics (IIAI-AAI-Winter)* (pp. 136–141). IEEE. https://doi.org/10.1109/IIAI-AAI-Winter64350.2024.00034
61. Vacha, L., & Barunik, J. (2012). Co-movement of energy commodities revisited: Evidence from wavelet coherence analysis. *Energy Economics*, *34*(1), 241–247. https://doi.org/10.1016/j.eneco.2011.10.007
62. Villar-Rubio, E., Huete-Morales, M. D., & Galán-Valdivieso, F. (2023). Using EGARCH models to predict volatility in unconsolidated financial markets: The case of European carbon allowances. *Journal of Environmental Studies and Sciences*, *13*(3), 500–509. https://doi.org/10.1007/s13412-023-00839-4
63. Zakeri, B., Staffell, I., Dodds, P. E., Grubb, M., Ekins, P., Jääskeläinen, J., Cross, S., & Rinne, E. (2023). The role of natural gas in electricity prices in Europe. *Energy Reports*, *10*, 2778–2792. https://doi.org/10.1016/j.egyr.2023.09.055
64. Zerbib, O. D. (2025). The effect of pro-environmental preferences on bond prices: Evidence from green bonds. In *Handbook of quantitative sustainable finance* (pp. 410–448). Chapman and Hall/CRC.

65. Zhang, R. (2025). Green finance and ESG investment strategies under climate risk management. *Economics and Management Innovation*, *2*(1), 140–148. https://doi.org/10.62051/emi.v2i1.42
66. Zhang, Y., & Umair, M. (2023). Examining the interconnectedness of green finance: An analysis of dynamic spillover effects among green bonds, renewable energy, and carbon markets. *Environmental Science and Pollution Research*, *30*(31), 77093–77109. https://doi.org/10.1007/s11356-023-27715-x
67. Zhou, G. (1993). Asset-pricing tests under alternative distributions. *The Journal of Finance*, *48*(5), 1927–1942. https://doi.org/10.1111/j.1540-6261.1993.tb05135.x

About authors

Eugenijus Gabrielius Ivanauskas is a first-year Master's student in Mathematics at the same faculty. In 2025, he completed his Bachelor's degree in Econometrics at Vilnius University, graduating cum laude. His main interests include mathematical modelling, statistics, and financial risk, which he plans to further develop through PhD studies after 2027. Alongside the studies, he works at Danske Bank in Model Risk Management, where he validates quantitative models related to financial risk, including ISDA SIMM, Value-at-Risk models for asset management, and CLO pricing frameworks. His experience combines a solid theoretical background with practical applications in finance.

Liepa Urbonaitė is a second-year Bachelor's student in Data Science at Vilnius University. Her primary academic interests lie in mathematics and statistics, which form the core of her studies and future aspirations. She plans to further deepen her knowledge in these areas through Master's studies. Alongside her academic work, she is employed as a tutor, teaching chemistry, mathematics, and physics. This role allows her to strengthen her analytical thinking while helping others build a solid foundation in scientific subjects. Her experience reflects a strong combination of theoretical understanding and practical application in problem-solving. She is also a recipient of multiple national awards in chemistry and has represented Lithuania in international competitions, earning bronze and silver medals at the International Junior Science Olympiad and the European Olympiad of Experimental Sciences.

Saulius Jokubaitis is an assistant professor at Vilnius University, Institute of Applied Mathematics, Faculty of Mathematics and Informatics. He holds a PhD in Mathematics from Vilnius University. His research focus is machine learning, econometrics, time-series analysis and risk modelling. In addition to his academic work, he serves as a consultant in the financial sector, applying advanced risk modelling techniques to real-world business challenges.